

High-resolution coregistered intravascular imaging with integrated ultrasound and optical coherence tomography probe

Xiang Li,¹ Jiechen Yin,² Changhong Hu,¹ Qifa Zhou,^{1,a)} K. Kirk Shung,¹ and Zhongping Chen^{2,3,a)}

¹Department of Biomedical Engineering, NIH Ultrasonic Transducer Resource Center, University of Southern California, Los Angeles, California 90089, USA

²Department of Biomedical Engineering, University of California, Irvine, California 92697, USA

³Beckman Laser Institute, University of California, Irvine, California 92612, USA and Edwards Lifesciences Center for Advanced Cardiovascular Technology, University of California, Irvine, California 92697, USA

(Received 5 May 2010; accepted 7 September 2010; published online 27 September 2010)

We report an integrated ultrasound (US) and optical coherence tomography (OCT) probe and system for intravascular imaging. The dual-function probe is based on a 50 MHz focused ring US transducer, with a centric hole for mounting OCT probe. The coaxial US and light beams are steered by a 45° mirror to enable coregistered US/OCT imaging simultaneously. Lateral resolution of US is improved due to focused ultrasonic beam. Mirror effects on US were investigated and *in vitro* imaging of a rabbit aorta has been carried out. The combined US-OCT system demonstrated high resolution in visualizing superficial arterial structures while retaining deep penetration of ultrasonic imaging. © 2010 American Institute of Physics. [doi:10.1063/1.3493659]

High frequency ultrasound (US) is a commonly used noninvasive medical imaging diagnostic method, which is usually operated in the pulse-echo mode, where amplitudes and time delays of backscattered ultrasonic waves are measured to generate a cross-sectional image. The working frequency for medical US is normally from 20–60 MHz in dermatology; 10–60 MHz in ophthalmology; and 20–50 MHz in intravascular ultrasound (IVUS), which allow spatial resolution from 30 to 400 μm .¹ For IVUS application, a side-looking unfocused single element transducer is the predominant design, which leads to a radial imaging geometry of the cross section of a vessel when mechanically scanned. The advantages of US as a popular means for intravascular imaging stem from its large penetration depth and moderate resolution in resolving plaque, lipid pool, and vessel structures.^{1,2} In addition, blood serves as a nature coupling median for US, rather than an obstruction for optical modalities.² However, the insufficient resolution of US imaging becomes a major limitation in characterizing certain critical microstructures of atheromatous plaque, for example, an accurate estimation of cap thickness of fibrous plaque in thin-cap fibroatheroma (TCFA), a disease which accounts for ~80% of sudden cardiac death.³ On the other hand, optical coherence tomography (OCT) is an optical-based modality for high-resolution, cross-sectional, and real-time imaging.^{4,5} OCT is analogous to B-mode US except that infrared light is used instead of ultrasonic waves.⁵ In OCT, a technique known as low-coherence interferometry is applied to measure the time delay of backscattered infrared light instead of measured electronically as in US.⁴ OCT has been used for atherosclerosis evaluation and shown to provide valuable information about microscopic features.^{2,5-7} However, the limited penetration depth (1–2 mm) prevents OCT from imaging the whole depth of a large lipid pool of a plaque.

Meanwhile, saline is needed for blood clearance in the clinical settings.²

Since the two modalities possess complimentary properties to each other, where OCT's high resolution could resolve superficial microstructures and US could penetrate the whole depth of vessel wall, an integrated imaging system combining the two would be more beneficial than either alone. Moreover, a minimal amount of flushing saline would be needed for OCT since US can serve as guidance while searching for targets in the blood vessel. The feasibility of combining information from intravascular OCT and US for detecting TCFA has been studied by several investigators,² who acquired US and OCT images from separate systems. The results indicated that neither modality alone is sufficient for detecting TCFA, while the combined use of OCT and IVUS provides much better sensitivity and specificity for evaluating TCFA. However, using two separate systems is time consuming, which requires patients endure extra suffer. Moreover, separately acquired US and OCT images may not be fully coregistered, which could result in inaccurate diagnosis.

In this paper, we report on an integrated dual-function US and OCT (US-OCT) probe and imaging system. Based on a high-frequency ring transducer, which allows a focused US beam and a light beam to be launched coaxially toward a common imaging spot, the hybrid probe demonstrated the capability of producing automatically coregistered US and OCT images simultaneously. As only one probe needs to be manipulated, the operating time is tremendously reduced compared to use US and OCT separately. In addition, the lateral resolution of US image is greatly improved by using a focused high-frequency transducer. *In vitro* imaging of a normal rabbit aorta was carried out with this US-OCT system. The results demonstrated the superiority of the coaxial probe design and its potential application in diagnosis and characterization of atherosclerotic plaques.

The schematic of the dual-modality probe that combines US transducer and OCT optical components is shown in

^{a)}Authors to whom correspondence should be addressed. Electronic addresses: qifazhou@usc.edu and z2chen@uci.edu.

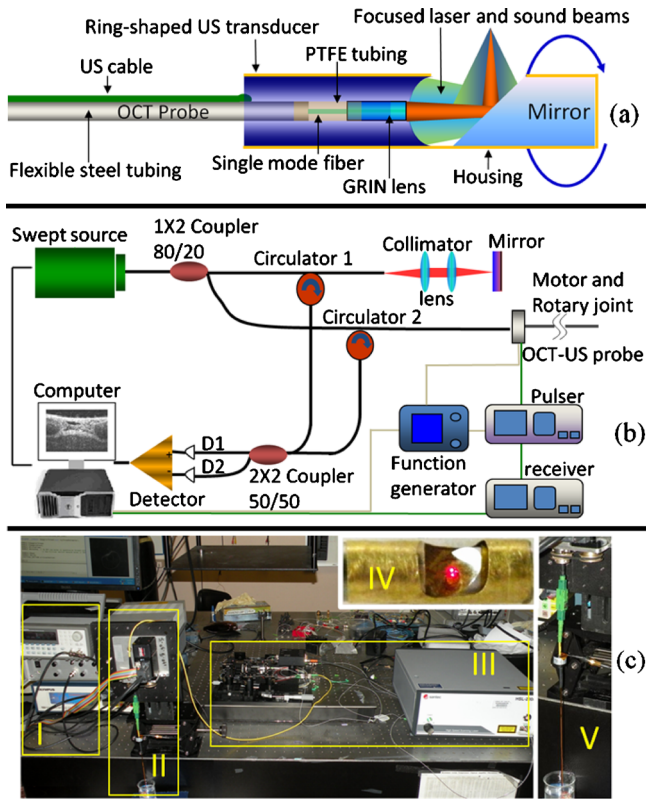


FIG. 1. (Color online) Schematic of US-OCT probe (a) and imaging system (b). Photograph of the US-OCT system (c): I, US subsystem; II, motor and rotary joint device; III, OCT subsystem; IV, close-up of the hybrid probe (visible light was used here for photograph); and V, close-up of the probe assembled to rotary joint device.

Fig. 1(a). The home-made 50 MHz focused ring transducer has an effective aperture of 2 mm outer diameter with a 0.8 mm hole at the center to make room for the OCT probe which has an outer diameter of 0.7 mm. The coaxial US and light beams have a common focal length of 4 mm, and both are steered into tissue by a 45° mirror along their pathway. The glass mirror, coated with aluminum, is fixed close to the anterior surface of the hybrid probe to ensure both beams are focused at tissue target. The mirror and hybrid probe are properly aligned and packaged in a brass tube housing on which a window is made to allow US and light beams to exit. After packaging, the monolithic US-OCT probe has a maximum outer diameter of 2.5 mm. The probe is then connected to a step motor and rotary joint device to enable rotational scanning inside a lumen. The rotary joint device consists of a fiberoptic rotary joint (Princeton, Inc., Pennington, NJ) and an electrical slip ring (Prosperous. Co. Hangzhou, China), which are used to transmit optical and electrical signals between rotary and stationary parts of the system.

The integrated US-OCT system is shown in Figs. 1(b) and 1(c). In the US part, a single sinusoidal wave centered at 50 MHz is generated by a pulser (Avtech Electrosystems Ltd., Ontario, Canada) to excite the transducer. Echo signal is received by a broadband receiver (Olympus NDT, Inc., Kennewick, WA) then digitized at the sampling rate of 400 MHz. A function generator provides 4 KHz trigger signals to both the pulser and the data acquisition board. The function generator is triggered by the step motor which is controlled by computer to synchronize the US and OCT imaging. For the swept-source (SS) OCT system,⁸ light from

a SS (center wavelength, 1310 nm; full width at half maximum bandwidth, 100 nm; output power, 2.7 mW; scanning rate, 20 kHz; Santec Corp., Komaki, Aichi, Japan) is split by an 80/20 1×2 coupler, with 80% of the power directed to the OCT-US probe and the remaining 20% to the reference arm. Two circulators are used in both arms to redirect back-scattered and backreflected light to the two input ports of a 50/50 2×2 coupler for balanced detection. The detected OCT signal is digitized at a sampling rate of 33 MHz.

In order to determine the performance of US subsystem, especially the mirror reflecting effects on the propagation of ultrasonic beams, a series of measurements were performed and showed that there was slightly loss in energy or change in beam profile. As an ultrasonic wave encounters an interface between two media, the directions of reflected and refracted waves are governed by Snell's law.^{9,10} The incident critical angle (θ_{ic}) of total internal reflection are defined as $\theta_{ic} = \sin^{-1}(c_1/c_2)$, where c_1 and c_2 are sound speeds in each medium. θ_{ic} at water and glass mirror interface can be calculated to be 15° . In our device, the incident angles of the focused sound beam with f number (focal length/aperture diameter) of two encountering a 45° mirror are calculated to be between 31° and 59° , which are much greater than θ_{ic} . Thus, "total internal reflection" occurs at the interface of water and mirror, or there is no propagation loss due to refraction or shear wave mode conversion.¹⁰ However, in B-mode US, images are acquired in pulse-echo mode. Ideally, US echo would return along the same pathway as incident wave, or total internal reflection also occurs for echo wave, which was further investigated.

To evaluate the mirror effects on the two-way propagation of ultrasonic wave, several tests without/with a mirror were carried out. First, pulse-echo¹¹ and two-way insertion loss¹¹ measurements were conducted. Comparing results without/with a mirror, no significant difference in center frequency (51/50 MHz), fractional bandwidth (58/58%), or sensitivity ($-24/-25$ dB) are observed. Next, to determine the US subsystem's spatial resolution, the linearly B-scan images of five $6 \mu\text{m}$ diameter tungsten wires were examined, which could be treated as ideal line targets since they were much thinner than the average US wavelength ($30 \mu\text{m}$). US images of wire phantoms without/with a mirror are shown in Figs. 2(a) and 2(d). The two images clearly demonstrate that the US beams are still focused at the designed focal point (4 mm) after reflected by the glass mirror. Figures 2(b), 2(c), 2(e), and 2(f) display the envelopes of the radio frequency (RF) signals acquired from the wires located at transducer's focal point. US axial (R_{axial}) and lateral (R_{lateral}) resolutions are determined from the -6 dB envelope width. Without a mirror reflection, R_{axial} and R_{lateral} are $25 \mu\text{m}$ and $48 \mu\text{m}$, respectively; while with a mirror reflection, those are 22 and $44 \mu\text{m}$, remain almost unchanged. Both situations are consistent with the theoretical values of 25 and $45 \mu\text{m}$ for a ring transducer. (Theoretically: $R_{\text{axial}} = c/(2BW)$;¹ $R_{\text{lateral}} \approx 0.75\lambda f/d$;¹⁰ where c is sound velocity in water; BW is (-6 dB) bandwidth; λ is average wavelength; f is focal length; and d is outer diameter of transducer aperture.)

For the OCT part of the integrated imaging system, the axial and lateral resolutions were optimized and measured to be 8 and $20 \mu\text{m}$,¹² which are much better than those of an US system.

In order to demonstrate the feasibility of the integrated

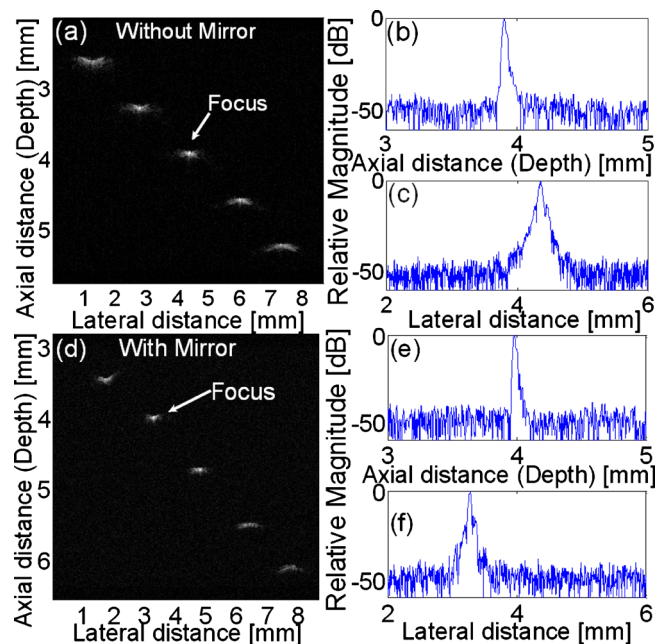


FIG. 2. (Color online) US wire phantom images without a mirror (a) and with a mirror (d), displayed with a dynamic range of 50 dB; axial and lateral envelopes of the RF echo signals from the wire located at transducer focal point without a mirror [(b) and (c)] and with a mirror [(e) and (f)].

US-OCT system in intravascular imaging, an *in vitro* study of a healthy rabbit aorta was performed. The aorta (only vascular) was fixed in 10% formalin for 24 h and preserved in phosphate buffer. During the experiment, the aorta was pinned to a piece of cork and immersed into saline. The results are shown in Fig. 3. It is not surprising that OCT image [Fig. 3(a)] resolves the inner profile of aorta more precisely and offers much higher resolution (smaller speckles) than US image [Fig. 3(b)]. However, only about 500 μm

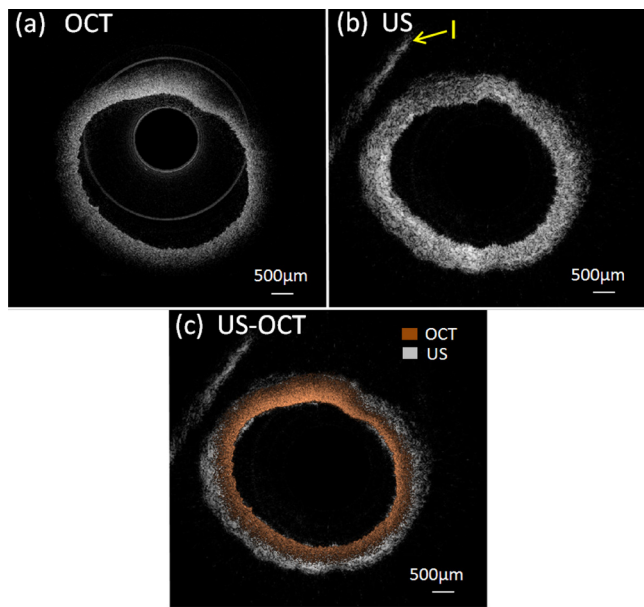


FIG. 3. (Color online) OCT (a), US (b), and combined US/OCT (c) images of a rabbit aorta. I: cork holder.

depth could be visualized in OCT image. On the other hand, US image provides a full-depth cross-section image of the aorta—even the cork used to position the aorta can be seen (region I) but with inferior resolution compared to OCT. A combined US-OCT image is displayed in Fig. 3(c), which clearly demonstrated the advantage in high resolution of OCT and deep penetration of US, which can offer complementary information for atherosclerosis diagnosis that cannot be obtained by either modality alone. Meanwhile, the similar shapes of OCT and US images illustrates the superiority in depicting coregistered intravascular images of the coaxial hybrid probe design and integrated imaging system.

In conclusion, we have presented a concept and the realization of an integrated US-OCT imaging system for intravascular imaging. Based on a 50 MHz focused ring transducer, the coaxial design of ultrasonic and light beam of the dual-modality probe can provide coregistered US and OCT imaging at the same time. Meanwhile, the lateral resolution of US image is improved greatly compared to conventional unfocused IVUS transducer. *In vitro* images of rabbit aorta were acquired using this imaging system. The results well demonstrate its feasibility in intravascular imaging and potential in atherosclerotic plaque characterization. The combination of US and OCT functions into one imaging system enable it to possess the advantages both in penetration depth and resolution at the same time, which would significantly reduce the physician's operating time and increase diagnostic accuracy compared to using separate probes.

We would like to thank Dr. Jonathan Cannata and Mr. Wei Wei for their help in this work. This project has been supported by the NIH grants (Grant Nos. EB-10090, RR-01192, EB-00293, and P41-EB2182). Mr. Xiang Li and Ms. Jiechen Yin have equal contributions to this paper and should be treated as cofirst authors.

- ¹F. S. Foster, C. J. Pavlin, K. A. Harasiewicz, D. A. Christopher, and D. H. Turnbull, *Ultrasound in Med. Biol.* **26**, 1 (2000).
- ²T. Sawada, J. Shite, H. M. Garcia-Garcia, T. Shinke, S. Watanabe, H. Otake, D. Matsumoto, Y. Tanino, D. Ogasawara, H. Kawamori, H. Kato, N. Miyoshi, M. Yokoyama, P. W. Serruys, and K. Hirata, *Eur. Heart J.* **29**, 1136 (2008).
- ³F. D. Kolodgie, A. P. Burke, A. Farb, H. K. Gold, J. Y. Yuan, J. Narula, A. V. Finn, and R. Virmani, *Curr. Opin. Cardiol.* **16**, 285 (2001).
- ⁴D. Huang, E. A. Swanson, C. P. Lin, J. S. Schuman, W. G. Stinson, W. Chang, M. R. Hee, T. Flotte, K. Gregory, C. A. Puliafito, and J. G. Fujimoto, *Science* **254**, 1178 (1991).
- ⁵P. Patwari, N. J. Weissman, S. A. Boppart, C. J. Jesser, D. Stamper, J. G. Fujimoto, and M. E. Brezinski, *Am. J. Cardiol.* **85**, 641 (2000).
- ⁶M. Kawasaki, B. E. Bouma, J. Bressner, S. L. Houser, S. K. Nadkarni, B. D. MacNeill, I. K. Jang, H. Fujiwara, and G. J. Tearney, *J. Am. Coll. Cardiol.* **48**, 81 (2006).
- ⁷G. J. Tearney, I. K. Jang, and B. E. Bouma, *J. Biomed. Opt.* **11**, 021002 (2006).
- ⁸J. P. Su, J. Zhang, L. F. Yu, H. G. Colt, M. Brenner, and Z. P. Chen, *J. Biomed. Opt.* **13**, 030506 (2008).
- ⁹K. K. Shung, *Diagnostic Ultrasound: Imaging and Blood Flow Measurements* (Taylor & Francis Group, Boca Raton, 2006), pp. 17–54.
- ¹⁰R. S. C. Cobbold, *Foundations of Biomedical Ultrasound* (Oxford University Press, New York, 2007), pp. 51–180.
- ¹¹J. M. Cannata, T. A. Ritter, W. H. Chen, R. H. Silverman, and K. K. Shung, *IEEE Trans. Ultrason. Ferroelectr. Freq. Control* **50**, 1548 (2003).
- ¹²J. C. Yin, H. C. Yang, X. Li, J. Zhang, Q. F. Zhou, C. H. Hu, K. K. Shung, and Z. P. Chen, *J. Biomed. Opt.* **15**, 010512 (2010).